11th Brazilian Congress on Manufacturing Engineering
May 24th-26th, 2021, Curitiba, PR, Brazil

DLP ADDITIVE MANUFACTURING OF CERAMICS: PHOTOSENSITIVE PARAMETERS, THERMAL ANALYSIS, POST-PROCESSING, AND PARTS CHARACTERIZATION

Italo Leite de Camargo
Institute of Education, Science and Technology of São Paulo - IFSP. Primeiro de Maio, 500. Itaquaquecetuba, SP, Brazil.
Department of Mechanical Engineering- EESC/USP. Trabalhador São Carlense, 400. São Carlos, SP, Brazil.
italo.camargo@ifsp.edu.br; italo.camargo@usp.br.

Rogério Erbereli
João Fiore Parreira Lovo
Carlos Alberto Fortulan
Department of Mechanical Engineering- EESC/USP. Trabalhador São Carlense, 400. São Carlos, SP, Brazil.
rogerio.erbereli@usp.br; joao.lovo@usp.br; fortulan@usp.br.

Abstract. *Digital light processing (DLP) is an additive manufacturing (AM) process that can produce high-performance ceramic parts with tiny structures, high dimensional precision, and outstanding surface quality. Curing the suspension to form the layers and the post-processing are important aspects to generate parts with good geometrical accuracy and mechanical properties. In this work, the photosensitive parameters and the thermal decomposition of a recently developed photosensitive ceramic suspension were investigated, creating a foundation for the manufacture of zirconia parts. It was found that the absorbance of the photoinitiator BAPO fits the exposure irradiance of a standard mercury vapor lamp from a commercial projector. Finally, ceramic test specimens were manufactured in a custom-built DLP 3D-printer, debound, and sintered at different temperatures (1400, 1500, and 1600 °C) for 2 hours to compare shrinkage, relative density, and flexural strength. For all temperatures, the shrinkage in the Z direction was found to be higher than in the XY plane. Parts sintered above 1500 °C presented a relative density greater than 95%. There is a tendency of increasing flexural strength with increasing temperature in the studied range and some parts sintered at 1600 degrees exceeded 200 MPa. However, a few specimens failed at the layers interface, causing a great variation in the flexural strength obtained.*

Keywords: *digital light processing, additive manufacturing, ceramics, 3D printing, vat photopolymerization*

1. INTRODUCTION

Additive manufacturing (AM) can produce small series complex ceramic parts without the high costs of molds (Schwentenwein; Homa, 2015; Zhang et al., 2020). Although several AM processes can manufacture ceramic parts, few of them can produce them with good mechanical properties, among which the vat photopolymerization processes (VP) can be highlighted (Wang, 2013). This type of AM, in which photosensitive liquid in a vat is selectively cured by light-activated polymerization (ISO, 2015), also stands out for its ability to produce tiny structures with high dimensional precision and good surface quality (Lian et al., 2017; Santoliquido et al., 2019). In addition, Digital light processing (DLP) is a VP process that produces the entire layer at once by projecting the section, being faster than VP processes based on the scanning of the region to be polymerized (Gibson et al 2015; Lian et al., 2017).

The VP of ceramics parts starts with the formulation and slurry preparation. It must have a high ceramic loading to avoid cracks (Griffith; Halloran, 1996) and delamination during post-processing (Jang et al., 2019) and proper rheological behavior and stability to allow uniform and homogeneous layers to be formed and so specifications of the ceramic particles, monomers and dispersants should be considered (Camargo et al., 2021a). Also, a suitable photoinitiator, compatible with the chosen monomers and light source must be selected (Gonzalez et al., 2019; Park et al., 2018).

Also, understanding the curing behavior of the photosensitive suspensions is another important aspect to ensure the geometrical accuracy and good mechanical properties in the ceramic parts manufactured by VP (Wei et al., 2019). The photopolymerizable ceramic suspensions generally follow the Beer-Lambert Law (Chen et al., 2019; Griffith; Halloran, 1996; Hinczewski et al., 1998a; Sun et al., 2019), described by Eq. 1

$$C_d = S_d \, ln(^{E}/_{E_c}) \tag{1}$$

Where C_d is the cure depth, S_d is the sensitivity of the suspension, also called penetration depth, E is the incident light energy density, and E_c is the critical energy (the minimum energy density initiate polymerization for a suspension).

The penetration depth and the critical energy are photosensitive parameters of the suspension and thus are a reference for the performance of these materials (Chen et al., 2019). They can be determined, using Eq. 1, by fitting experimental data the relationship between the incident light and the cure depth. The calculation of such parameters provides information for determining printing conditions as exposure energy, which should provide a cure depth larger than the layer thickness to ensure proper adhesion between the layers (Borlaf et al., 2019; Hu et al., 2018; Komissarenko et al., 2018; Li; Zhao, 2017). Therefore, delamination is avoided (Borlaf et al., 2019; Chen et al., 2019; Wei et al., 2019) and parts with good mechanical properties can be generated (Wei et al., 2019). On the other hand, excessive energy exposure lead to over-polymerization and a decrease in the process accuracy (Borlaf et al., 2019; Wei et al., 2019).

Moreover, the post-processing of the green printed parts is a key factor in the success of manufacturing these parts. The debinding is a critical step in the VP additive manufacturing of ceramics and adequate heating rates during this stage are necessary to avoid cracks (Johansson et al., 2017; Komissarenko et al., 2018) as well as the sintering temperature has an important influence on the properties of the final parts (Azarmi; AmirI, 2019; Liu et al., 2020; Varghese et al., 2018; Wu et al., 2018; Xing et al., 2020).

In this work, the photosensitive parameters and the thermal decomposition of a recently developed photosensitive ceramic suspension (Camargo et al., 2021b) were investigated, ceramic test specimens were manufactured in a custom-built DLP 3D-printer, debound and sintered at different temperatures and shrinkage, relative density, and flexural strength of these parts were investigated.

2. MATERIALS AND METHODS

A ceramic photosensitive slurry was prepared and its photosensitive parameters and thermal decomposition were evaluated. Next, ceramic pasts were manufactured by DLP additive manufacturing and post-processed and finally characterized, as described next.

2.1 Slurry preparation

The photosensitive ceramic slurry was prepared based on the formulation proposed by Camargo et. al. (2021b). Thus, partially stabilized zirconia powder (TZ-3Y-E, Tosoh Corporation, Japan), the monomer Poly(ethylene glycol) diacrylate, (PEGDA 250, Sigma Aldrich, USA), the photoinitiator Phenylbis(2,4,6-trimethylbenzoyl)phosphine oxide (PPO, Sigma Aldrich, USA), and the dispersant DISPERBYK-111 (BYK-Chemie, Germany) were mixed and ball-milled for 24 hours to break up agglomerates and homogenize the suspension with 40 vol% ceramic loading. Such slurry presents rheological behavior and stability suitable for the process (Camargo et al., 2021b).

2.2 Additive manufacturing and light source irradiance

Ceramic parts with 100 μm layer thickness were manufactured in a custom-built top-down DLP 3D printer which uses a recoating system for DLP 3D Printers composed of two blades with sequential action (Camargo et al., 2020) and a commercial projector with a mercury vapor lamp that had its UV filter removed. In order to check compatibility with the chosen photoinitiator and calculate the useful irradiance, the emission spectrum of this lamp was obtained using a Fiber Optic UV-Vis Spectrometer (USB4000, Ocean Optics) which was positioned in the 3D printer where the formation of layers occurs.

2.3 Photosensitive parameters

Photosensitive parameters (penetration depth Dp and critical exposure energy Ec) were determined by the relationship between curing thickness and exposure energy to the light source. For this purpose, the photopolymerizable suspensions were poured into a petri dish and positioned in the DLP equipment. The slurries were cured with different exposure times. The layers were rinsed with isopropyl alcohol (IPA) and their thickness was measured using a caliper, similar to what is described in the literature (Chen et al., 2019; Hu et al., 2018) and the photosensitive parameters were determined by fitting the experimental data to the Beer-Lambert Law.

2.4 Thermal analysis

In order to define the debinding process, the thermal decomposition of the ceramic green parts was analyzed by thermogravimetric analysis (SDT Q600, TA Instruments). The parts were heated (10°C/min) from room temperature to 1000 °C in air (50 mL/min).

2.5 Post-processed parts characterization

The printed parts were rinsed with isopropyl alcohol (IPA) and dried on the oven for 12 h at 100 °C. The samples were debound and sintered at different temperatures (1400, 1500, and 1600 °C) for 2 hours in a box furnace (Blue M, Lindberg) in air environment. The density of the sintered parts was measured based on Archimedes' Principle using an analytical balance with resolution 0,01 mg (AUW220D, Shimadzu). Flexural three-point strength tests were performed on printed bars (25 mm x 2 mm x 1.5 mm) using a universal testing machine (Bionix, MTS®) with a load cell of 15 kN, a span of 20 mm, and a crosshead speed of 0.2 mm/min

3. RESULTS AND DISCUSSION

The investigation of the photosensitive parameters and thermal decomposition of the photosensitive ceramic suspension created a foundation for the successful additive manufacturing and post-processing of zirconia parts, as described in this section.

3.1 Light source irradiance

Most related works use either laser (Hinczewski et al., 1998b; Li; Zhao, 2017; Sun et al., 2019) or monowaved led (Johansson et al., 2017; Komissarenko et al., 2018; Wu et al., 2019) centered at a specific wavelength that overlaps the absorption range of the initiator. Conversely, this works uses a standard mercury vapor lamp from a commercial projector with most of the emission in visible light, which highlights the process of choosing the photoinitiator. Among the most used photoinitiator for ceramic sensitive suspensions, 1-Hydroxycyclohexyl phenyl ketone (Irgacure 184 or HCPK) does not respond and Diphenyl(2, 4, 6-trimethylbenzoyl) phosphine oxide TPO has a small absorption in long wave UV. On the other hand, phenylbis(2,4,6-trimethyl benzoyl)phosphine oxide (Irgacure 819, BAPO, or PPO) stands out for its effective absorption up to 420 nm (Bertolo et al., 2017; Green, 2010; Wei et al., 2020), thus justifying its selection for use with the mentioned light source. Figure 1 shows the absorbance graph of BAPO (Green, 2010) and the measured emission spectrum of the mercury vapor lamp, which delivers approximately 7.9 mW/cm^2 with a broad emission spectrum (380-800 nm), of which just 0.5 mW/cm^2 is useful irradiance

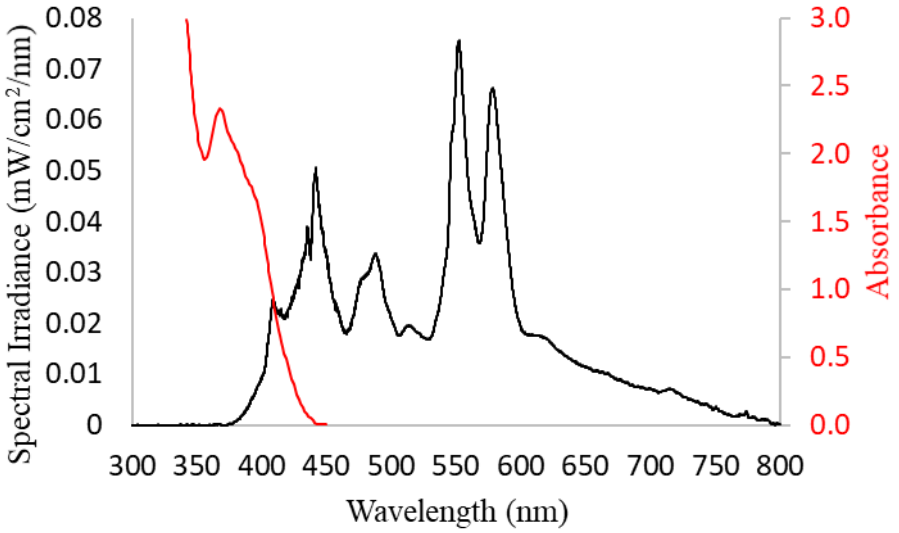

Figure 1. Emission spectrum of the used mercury vapor lamp and absorbance of the photoinitiator selected (BAPO)

3.2 Photosensitive parameters

Figure 2 shows the relation between the cure depth and exposure energy. The critical energy found (1.78 mJ/cm^2) is comparable with the lowest values obtained in the literature for photosensitive ceramic suspensions (Chen et al., 2019; Wu et al., 2019). In the DLP AM, the cure depth is a key factor for the interlayer combination (Li; Zhao, 2017) and it should be higher than the layer thickness to provide sufficient layer integration (Borlaf et al., 2019; Johansson et al., 2017; Wei et al., 2019). On the other hand, if cure depth is too high the accuracy will be impaired and so it should be at 1.1 to 1.35 times the layer thickness (Wei et al., 2019). Thus, for the AM of ceramic parts with 100 µm layer thickness, the exposure time was set to 10 mJ/cm^2.

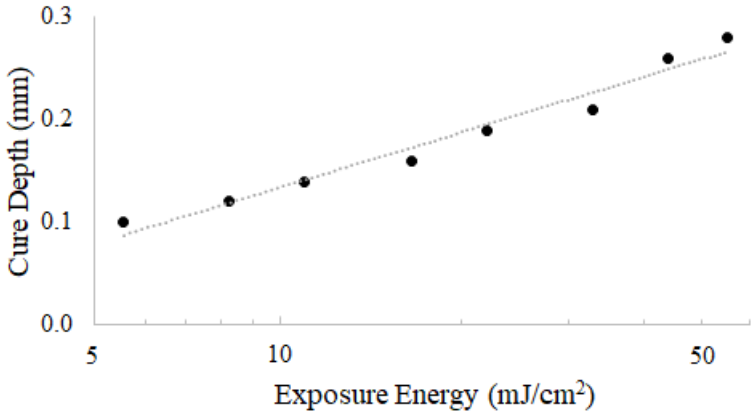

Figure 2. Cure depth vs exposure energy of the photosensitive ceramic suspension

3.3 Thermal Analysis

The thermogravimetric analysis is shown in Figure 3a. The total weight loss was 23.4% and no mass change was recorded after 600 °C. It can be seen that decomposition rates are higher between 350 and 470 °C (18.0% of weight loss) with a maximum peak at 400 °C. Using the thermal analysis, the debinding and sintering program was defined. The heating rate was reduced for higher decomposition rates and a hold point was introduced at the maximum peak temperature and other at 600 °C to ensure that all the organics were removed before the heating rate increase. Therefore, the parts were debound and sintered following the protocol (Figure 3b): 1 °C/min from room temperature to 350°C, 0.5 °C/min up to 600 °C with plateaus of 1 h at 400 °C and 600 °C, 5 °C/min up to 900°C and 6 °C/min up to the sintering temperature and held for 2 hours. Different sintering temperatures (1400, 1500, and 1600 °C) were evaluated in this work.

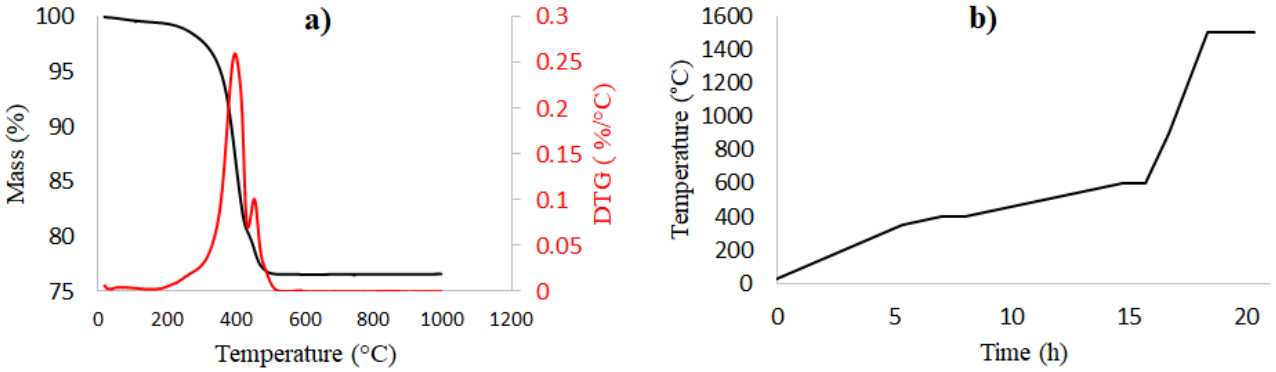

Figure 3. a) Thermogravimetric analysis of the green printed parts. b) Post-processing protocol

3.4 Post-processed parts characterization

DLP was used to manufacture not only specimens but also parts with tiny details as illustrated in Figures 4 and 5. Further, dense parts were obtained. The linear shrinkage and relative density of the sintered ceramic parts increased with increasing sintering temperature (Figure 6), and parts sintered at 1600 °C reached a relative density of 95.4% and their linear shrinkage exceeded 25% in all directions. The shrinkage in the building direction was always higher than in the XY plane, evidencing the anisotropic nature of the process.

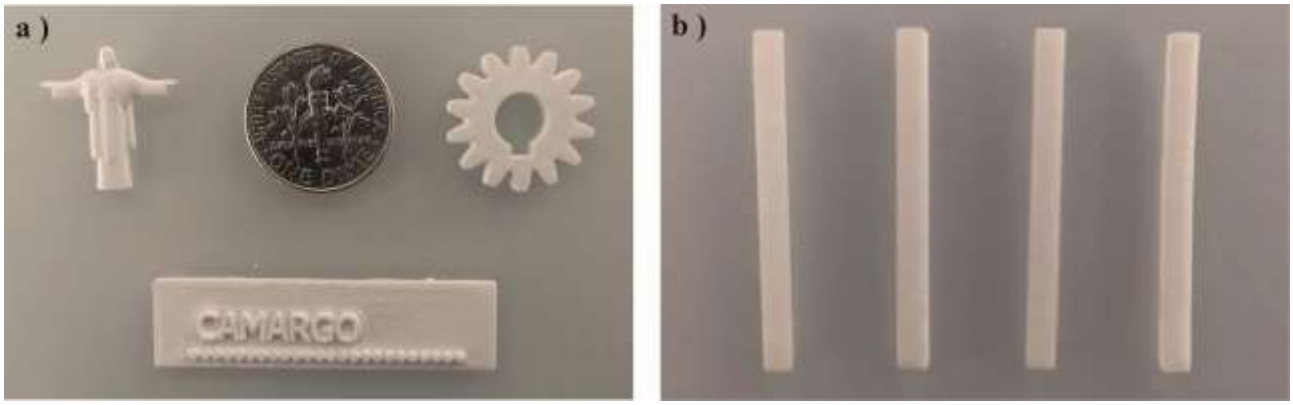

Figure 4. a) Green printed parts. b) Flexural specimens printed and sintered at 1500 °C.

Figure 5. Adaptation of Christ the Redeemer Statue (Rio de Janeiro – Brazil) printed and sintered at 1500 °C.

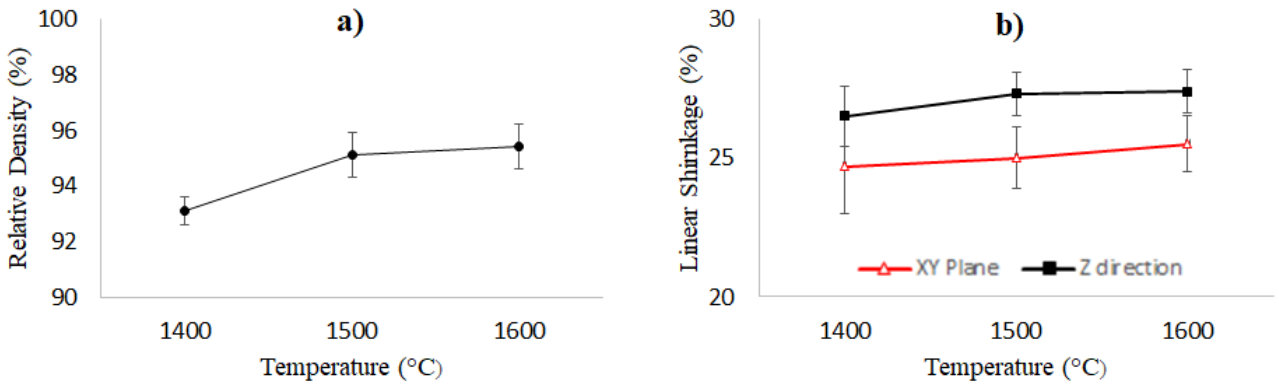

Figure 6. Characterization of printed parts sintered at different temperatures. a) Relative density. b) Linear Shrinkage

Finally, a tendency of increasing flexural strength with rising sintering temperature in the studied range can be observed in Figure 7a. Some parts sintered at 1600 degrees exceeded 200 MPa, which is still significantly less than the value obtained for zirconia produced by conventional processes. Some specimens failed at the layers interface (Figure 7b), causing a great variation in the flexural strength obtained. Decreasing the layer thickness, adding components to the formulation as plasticizers, and variations in the post-processing may be the subject of future work and help to improve the properties of ceramic parts manufactured by DLP additive manufacturing.

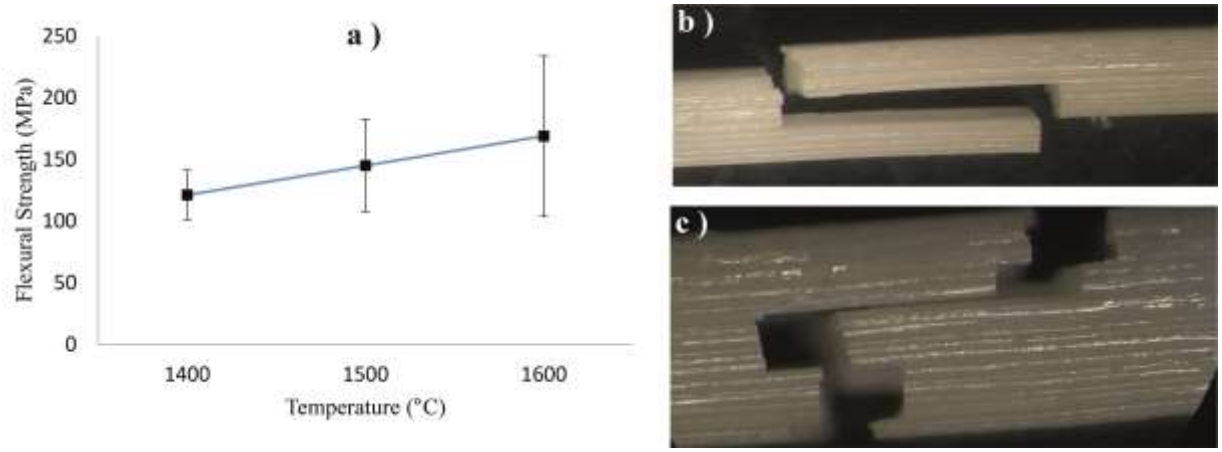

Figure 7. a) Flexural strength of the printed parts sintered at different temperatures. b) Specimens that failed at the layers interface in the flexural test.

4. CONCLUSIONS

In this work, a photosensitive ceramic suspension was prepared and characterized and its photosensitive parameters and the thermal decomposition were investigated in order to create guidelines to the manufacturing of ceramic parts such as the exposure energy per layer and the post-processing protocol. The selection of BAPO as the photoinitiator allowed ceramic parts to be manufactures in a custom-built DLP 3D-printer whose light source is a standard mercury vapor lamp from a commercial projector with most of the emission in visible light. The printed parts were sintered at different temperatures (1400, 1500, and 1600 °C). The shrinkage in the building direction was always higher than in the XY plane, evidencing the anisotropic nature of the process. The parts sintered at 1600 °C presented a density of 95.4% and some of these parts exceeded 200 MPa in flexural strength. However, some specimens failed at the layers interface and an investigation of how to alleviate this problem should be done in future works. The influence of changing layer thickness and the addition of components as plasticizers on the properties of ceramics parts fabricated by DLP additive manufacturing may also be subject of future works.

5. ACKNOWLEDGEMENTS

This study was financed in part by the Coordenação de Aperfeiçoamento de Pessoal de Nível Superior - Brasil (CAPES) - finance code 001

6. REFERENCES

Azarmi, F.; Amiri, A., 2019. "Microstructural evolution during fabrication of alumina via laser stereolithography technique". *Ceramics International*, Vol. 45, n. 1, p. 271–278.

Bertolo, M. V. L. et al., 2017. "Influence of photoinitiator system on physical-chemical properties of experimental self-adhesive composites". *Brazilian Dental Journal*, Vol. 28, n. 1, p. 35–39.

Borlaf, M. et al., 2019. "Development of UV-curable ZrO2 slurries for additive manufacturing (LCM-DLP) technology". *Journal of the European Ceramic Society*, Vol. 39, n. 13, p. 3797–3803.

Camargo, I. L. et al., 2020. "DLP 3D Printer with innovative recoating system". *Brazilian Technology Symposium (BTSym'20)*, 26-28 October, Pontifical Catholic University of Campinas, Campinas-SP, Brazil. Anais...

Camargo, I. L. et al., 2021a. "A review on the rheological behavior and formulations of ceramic suspensions for vat photopolymerization". *Ceramics International*, Vol. 47, n. 9, p.11906-11921. <https://doi.org/10.1016/j.ceramint.2021.01.031>.

Camargo, I. L. et al., 2021b. "3Y-TZP DLP additive manufacturing: solvent-free slurry development and characterization". *Materials Research*, v. In press. <https://doi.org/10.1590/1980-5373-MR-2020-0457>.

Chen, Z. et al., 2019. "Preparation of high solid loading and low viscosity ceramic slurries for photopolymerization-based 3D printing". *Ceramics International*, Vol. 45, n. 9, p. 11549–11557.

Gibson, I.; Rosen, D.; Stucker, B., 2015. *Additive manufacturing technologies: 3D printing, rapid prototyping, and direct digital manufacturing*. New York: Springer Science, 2nd edition.

Gonzalez, P. et al., 2019. "Additive Manufacturing of Functionally Graded Ceramic Materials by Stereolithography". *Journal of Visualized Experiments*, Vol. 143, e57943.

Green, W. A., 2010. Industrial Photoinitiators: A techinical guide. CRC Press - Taylor & Francis Group,

Griffith, M. L.; Halloran, J. W., 1996. "Freeform fabrication of ceramics via stereolithography". *J. Am. Ceram. Soc.*, Vol. 79, n. 10, p. 2601, 1996.

Hinczewski, C.; Corbel, S.; Chartier, T., 1998a. "Stereolithography for the fabrication of ceramic 3D parts". *Rapid Prototyping Journal*, Vol. 4, n. 3, p. 104–111.

Hinczewski, C.; Corbel, S.; Chartier, T., 1998b. "Ceramic suspensions suitable for stereolithography". *Journal of the European Ceramic Society*, Vol. 18, n. 6, p. 583–590.

Hu, K. et al., 2018. "Design of a Shaping System for Stereolithography with High Solid Loading Ceramic Suspensions". *3D Printing and Additive Manufacturing*, Vol. 5, n. 4, p. 311–318.

ISO/ASTM 52900, 2015, "Additive manufacturing — General principles — Terminology" Geneva.

Jang, K. J. et al., 2019. "Effect of the volume fraction of zirconia suspensions on the microstructure and physical properties of products produced by additive manufacturing". *Dental Materials*, Vol. 35, n. 5, p. e97–e106.

Johansson, E. et al., 2017. "Influence of resin composition on the defect formation in alumina manufactured by stereolithography". *Materials*, Vol. 10, n. 2.

Komissarenko, D. A. et al., 2018. "Rheological and curing behavior of acrylate-based suspensions for the DLP 3D printing of complex zirconia parts". *Materials*, Vol. 11, n. 12.

Li, K.; Zhao, Z. "The effect of the surfactants on the formulation of UV-curable SLA alumina suspension". *Ceramics International*, Vol. 43, n. 6, p. 4761–4767, 2017.

Lian, Q. et al., 2017. "Oxygen-controlled bottom-up mask-projection stereolithography for ceramic 3D printing". *Ceramics International*, Vol. 43, n. 17, p. 14956–14961.

Liu, X. et al., 2020. "The preparation of ZrO2-Al2O3 composite ceramic by SLA-3D printing and sintering processing". *Ceramics International*, Vol. 46, n. 1, p. 937–944.

Park, H. K. et al., 2018. "A visible light-curable yet visible wavelength-transparent resin for stereolithography 3D printing". *NPG Asia Materials*, Vol. 10, n. 4, p. 82–89.

Santoliquido, O.; Colombo, P.; Ortona, A., 2019. "Additive Manufacturing of ceramic components by Digital Light Processing: A comparison between the “bottom-up” and the “top-down” approaches". J*ournal of the European Ceramic Society*, Vol. 39, n. 6, p. 2140–2148.

Schwentenwein, M.; Homa, J., 2015. "Additive manufacturing of dense alumina ceramics". I*nternational Journal of Applied Ceramic Technology*, Vol. 12, n. 1, p. 1–7.

Sun, J.; Binner, J.; Bai, J., 2019. 'Effect of surface treatment on the dispersion of nano zirconia particles in non-aqueous suspensions for stereolithography". *Journal of the European Ceramic Society*, Vol. 39, n. 4, p. 1660–1667.

Varghese, G. et al., 2018. "Fabrication and characterisation of ceramics via low-cost DLP 3D printing". *Boletin de la Sociedad Espanola de Ceramica y Vidrio*, Vol. 57, n. 1, p. 9–18.

Wang, J., 2013. "A Novel Fabrication Method of High Strength Alumina Ceramic Parts Based on Solvent-based Slurry Stereolithography and Sintering". *International Journal Of Precision Engineering And Manufacturing*, Vol. 14, n. 3, p. 485–491.

Wei, L. Et Al., 2019. "A novel fabrication of yttria-stabilized-zirconia dense electrolyte for solid oxide fuel cells by 3D printing technique". *International Journal of Hydrogen Energy*, Vol. 44, n. 12, p. 6182–6191.

Wei, Y. et al., 2020. "Stereolithography-Based Additive Manufacturing of High-Performance Osteoinductive Calcium Phosphate Ceramics by a Digital Light-Processing System". *ACS Biomaterials Science and Engineering*, Vol. 6, n. 3, p. 1787–1797.

Wu, X. et al., 2019. "Influence of boundary masks on dimensions and surface roughness using segmented exposure in ceramic 3D printing". *Ceramics International*, Vol. 45, n. 3, p. 3687–3697.

Wu, Z. et al., 2018. "Research into the mechanical properties, sintering mechanism and microstructure evolution of Al2O3-ZrO2 composites fabricated by a stereolithography-based 3D printing method". *Materials Chemistry and Physics*, Vol. 207, p. 1–10.

Xing, B. et al., 2020. "Dense 8 mol% yttria-stabilized zirconia electrolyte by DLP stereolithography". *Journal of the European Ceramic Society*, Vol. 40, n. 4, p. 1418–1423.

Zhang, K., 2020. et al. "Digital light processing of 3Y-TZP strengthened ZrO2 ceramics". *Materials Science and Engineering A*, Vol. 774, p. 138768.

7. RESPONSIBILITY NOTICE

The authors are the only responsible for the printed material included in this paper.